Strength reduction for upheaval buckling of buried pipes in blocky clay backfill

Brennan, Andrew John ; Ghahremani, Mahmoud; Brown, Michael John

Published in:
Ocean Engineering

DOI:
10.1016/j.oceaneng.2016.12.006

Publication date:
2017

Strength Reduction for Upheaval Buckling of Buried Pipes in Blocky Clay Backfill

OE-D-16-00578-R1

Andrew John Brennan [a.] (corresponding author),

Mahmoud Ghahremani [b.]

Michael John Brown [c.]

[a.] a.j.brennan@dundee.ac.uk, School of Science and Engineering, University of Dundee, DUNDEE, DD1 4HN, UK

[b.] mahmoud879@gmail.com, formerly School of Science and Engineering, University of Dundee, DUNDEE, DD1 4HN, UK

[c.] m.j.z.brown@dundee.ac.uk, School of Science and Engineering, University of Dundee, DUNDEE, DD1 4HN, UK

Abstract

Offshore pipelines are often buried to protect the pipeline from external loads and upheaval buckling. Models for pipe uplift resistance in clay soils are based predominantly on homogenous backfill conditions. In practice, however, there will be significant soil disturbance during installation. With certain trenching techniques this may produce a backfill more akin to a matrix of lumps of intact soil connected by weaker remoulded interfaces. This research uses centrifuge modelling to assess the resistance provided by a representative lumpy clay backfill that has experienced self-weight consolidation. A model pipe is then uplifted through this model backfill in order to assess the soil uplift resistance. Results show that the uplift resistance in this material is governed strongly by the size of the lumps and, to a lesser extent, by the rate at which displacement occurs. When interpreted in terms of the strength reduction η, that may be used to correct between theoretical and measured uplifts, lower values were derived than those currently used based on intact soils. The value of η is seen to be controlled by a non-dimensional drainage parameter, but may be practically estimated based on an estimate of the size of lumps relative to the pipe diameter.

Keywords: pipeline geotechnics; upheaval buckling; centrifuge modeling; clay

1. Introduction

Offshore pipelines are often buried to protect the pipeline from external loads or to reduce thermal losses. However, if the depth of soil cover above the pipeline is insufficient then the pipe can buckle upwards to relieve thermal strains. It is therefore important to both ensure adequate depth of cover above a given pipeline and also to be able to reliably evaluate how much resistance this can provide should the pipeline attempt to uplift.

Recent years have seen many studies on prediction of uplift behaviour. These are largely divided between theoretical work e.g. (Maltby and Calladine, 1995; Martin and White, 2012), full-scale testing e.g. (Eiksund et al., 2013; Schaminee et al., 1990; Trautmann et al., 1985) and geotechnical centrifuge testing e.g. (Cheuk et al., 2007; Ng and Springman, 1994; Wang et al., 2009). This accumulated knowledge has fed into design codes such as that published by (DNV, 2007) which provide a framework for designers to best predict the likely performance of their pipelines. Much of the literature, however, relies on analysis and testing of a pipeline that has been wished-in-place. That is, there is no attempt to model disturbance of the insitu soil or backfill material caused during the installation process.

Installation may be undertaken using jetting where the soil is subjected to localised high water pressures facilitating a downwards settlement of the pipeline under gravity. Depending on the soil condition and the jet configuration, the soil may either be liquefied into a homogenously sedimenting mass of particles as examined by (Bransby et al., 2002), or it may be locally cut resulting in a matrix of lumps of relatively intact soil connected by a weaker reconsolidated material. Both of these mechanisms are highly disruptive to the condition of the soil and therefore allowance should be made that the soil conditions above the pipeline will not be the same as those of the in-situ soil in either case.

This research therefore aims to better understand the factors governing behaviour of a pipeline in a material that is more representative of conditions following a disruptive installation process. Of particular interest here is the case when the backfill is not homogenous but consists of intact lumps in a normally consolidated matrix, a “lumpy” or “blocky” backfill. This is achieved through physical model tests of a 1:25 scale small scale model pipe being uplifted through clay seabed of variously disturbed

condition. A range of uplift velocities were also tested (0.6 mm/hour, 6mm/hour, 60 mm/hour, prototype scale). In order to accelerate consolidation and to correctly match the in situ self-weight stresses of the soil to the larger prototype, the tests were performed on a geotechnical centrifuge with a gravitational field of 25g.

1.2 Interpretation Framework

In this work, the undrained soil behaviour framework is considered, in line with conventional treatment of clay soils. The literature listed above (and others) provides largely similar interpretations of uplift resistance, with the version provided by recommended practice document DNV-RP-F110 (DNV, 2007) used as the basis for this work. This is because this document provides some design commentary on incorporating installation effects into the design. In DNV-RP-F110, the upheaval behaviour of a pipe requires failure of the soil in either a local (Figure 1a) or a global failure mode (Figure 1b). As indicated by the governing equations presented in the DNV, the soil resistance to shearing in a global mode is less when the depth of cover H is low, so this is sometimes termed a "shallow" mechanism. However, as the global mechanism requires uplift of overlying soil mass plus shearing along a surface dependent on depth of cover then this becomes inefficient at greater depths, whereas the local mechanism is relatively insensitive to parameter H when considering undrained strengths. Of particular interest in this analysis is the local mechanism, because the formulation of the resistance of such pipes includes an empirical factor η that is intended to correct between measured data and theoretical estimates. The expression for peak uplift resistance R is given in Equation 1, where N_c is an analytically-derived bearing capacity factor, D is pipe diameter, s_u is the undrained strength of soil measured at the level of the pipe's centre and η is the empirical strength reduction factor.

$$R = N_c D s_u \eta \qquad \text{Equation 1}$$

As the pipe is unable to achieve a complete "flow-around" type mechanism until cover depths in excess of 4.5 D are achieved, the bearing capacity factor N_c is provided as in Equation 2, where parameter r is a roughness factor ranging from 0 in the perfectly smooth case to 1 for a perfectly rough pipe.

$$N_c = 2\pi\left[1+\frac{1}{3}\tan^{-1}\left(\frac{H+D/2}{D}\right)(1+r)\right] \qquad \text{Equation 2}$$

The commentary on trenching methods in (DNV, 2007) suggests that jetting causes the entire soil mass to go into suspension. Strength may therefore be modelled by assuming a reconsolidated (i.e. effective stress dependent) shear strength exists throughout if an adequate period of reconsolidation is allowed for strength regain and adequate reduction made to H to consider the reduced depth of cover due to consolidation. However, anecdotal evidence suggests that some soils (and some jetting and ploughing strategies) may not produce a homogenous backfill but a lumpy or blocky backfill as described above. Therefore the backfill becomes a matrix consisting of lumps of relatively intact soil connected by the relatively weaker reconsolidated soil, and the use of a very soft reconsolidated strength based on a very low effective stress of a homogenous soil mass may be unrepresentative.

Parameter η in Equation 1 accounts for differences between the design undrained shear strength s_u and the back-calculated value following testing in remoulded clays according to DNV. Such differences are described in this source as being due to rate and viscous effects, and progressive failure regime, but the factor could also be usable to examine apparent strength reductions due to trenching disturbance. Data presented in this work will therefore use the strength reduction factor η as a means for identifying the relative effect of having a lumpy material as backfill, rather than a completely uniform soil at either intact or remoulded strength. The rationale will be to complement the existing industry standard formulations rather than create new ones, as well as better explore the meaning of this parameter.

2. Centrifuge Testing

2.1 Equipment

As the blocky backfill material relies on both a coherent intact soil and an interstitial soil consolidated under correct effective stresses, small scale models tested without the additional gravity are unable to reach representative strengths. Therefore physical models for this study were tested on the 3m radius beam centrifuge at the University of Dundee. Spinning the 1:25 scale model such that the normal

acceleration field equals 25 times earth's gravity g makes the small soil mass weigh the same as one that was 25 times deeper, matching the effective stress fields in model and prototype. This has the benefit of enabling consolidation to occur at the correct stresses as well as at accelerated timescales. Further discussion of centrifuge scaling laws may be found elsewhere, e.g. (Schofield, 1980); all data presented here will be in prototype or normalized scales with comments on scaling where required.

The model pipe, as shown in Figure 2a, was 25.4 mm diameter (D), corresponding to 635 mm at prototype scale. The length was 234 mm, slightly less than the width of the model container in order to create plane strain conditions without friction at each end of the pipe. The model container width was 115 mm, leaving space for 1.8D of soil either side of the pipe which is sufficient to enable the formation of a displacement mechanism (Figure 1). Uplift at the desired speed was provided by a screw jack driven by a stepper motor, which pulled the pipe through a hanger connected to the two thin rods as shown in Figure 2a. To permit settlement of the pipe during the consolidation phase and eliminate potential hang-up of consolidating soil above a rigidly fixed pipe, the rods were able to move vertically downwards relative to the hanger. Load was measured above the hanger, with the buoyant weight of the pipe/hanger subtracted from measurements so that only soil resistance is presented.

To monitor pore pressures, two pressure transducers were installed inside the pipe body, which was machined to allow these to measure pore pressures at the crown and the bottom of the pipe as shown in Figure 2b. The two thin rods were hollow and open ended, to enable the transducers to access a reference pressure during testing.

2.2 Soil Preparation

The soil chosen for the study was formed from kaolin powder, of specific gravity G_s = 2.65, plastic limit 30% and liquid limit 75%. The dry powder was mixed with water at 125% water content using a mechanical mixer, and then poured into a cylindrical press. A nominal pressure of 240 kPa was applied to the press in four increments; later calculations showed that this was carried only partly by the soil and partly by the equipment, making the actual consolidation pressure less than 240 kPa. After two weeks of consolidation, the soil was unloaded in four stages and removed from the cylinder.

To quantify the shear strength of the “undisturbed” clay, a number of hand vane tests were carried out, giving a mean undrained shear strength of 7 kPa (± 1 kPa). These tests were carried out throughout the sample in the first instance, in case of local inhomogeneities in the sample, and subsequently on each new batch for quality control.

Three different lump sizes were created from these consolidated samples. Samples of each lump size are shown in Figure 3. “Big cubes” (Figure 3a) were made by slicing the consolidated sample into 25 mm layers, then manually cutting with a knife in order to produce cubes with each side being 25 mm (625 mm at prototype scale). This resulted in a cube with sides approximately similar dimensions to the dimeter of the pipeline (0.98D). “Small cubes” (Figure 3b) were made by slicing the consolidated sample into layers of 12 mm thickness, and then passing the resultant lamina through a prefabricated mesh, leaving cubes of clay with each side being 12 mm. This resulted in a cube with sides of 0.47D or prototype length of 300 mm. “Grated” lumps (Figure 3c) were made using a standard domestic catering cheese grater. The resulting lumps had a length of 30-40 mm (model scale), a width of 4-6 mm and a thickness of 2-3 mm, and represent the smallest lump size tested. As there is little information available on the size of actual lumps created in the field the cube sizes were selected such that cubes were of comparable dimensions to the pipeline (“Big cubes”) and the influence of cube size could be explored (“small cubes”). Grated lumps were used to investigate the effects of a very different geometry but also to overcome the practicalities of forming cubes with sides smaller than 12 mm. Further information on sample and lump preparation can be found in Ghahremani (2008).

2.3 Test Procedure

Model construction was carried out using a fixed mass (4.25 kg) of soil lumps for each test. The model container was first filled with water, then soil lumps were added to at least 25 mm (i.e. 1.D) at the base of the model before the pipe was added, so that it was surrounded by soil and was able to form a continuous mechanism involving soil below the pipe if required (Figure 1). The pipe was held in position upright while the rest of the lumps were added randomly by hand and allowed to settle freely through the water to represent the settlement that would occur after the lumps are cut from the seabed. Once the target mass of soil had been added, the actuator was attached to the hanger such

that settlement of the pipe could occur freely, and the model was loaded onto the centrifuge. The initial soil surface level was measured relative to the top of the centrifuge box and the pipeline load hanger. An LVDT was added above the load hanger in order to measure pipeline uplift displacements.

Once the centrifuge was accelerated up to the required 25g, this was held for a fixed period to simulate the self-weight consolidation of the soil lumps prior to the switching on of the pipeline. For tests presented here, a period of 1 month prototype scale was used; Ghahremani and Brennan (2009) showed that the enhanced compressibility of the lumpy material meant that consolidation periods of one month and three months produced soils that were materially the same in terms of measured results, and after 1 month the excess pore pressures measured by the transducers in the pipe had reduced to less than 6% of hydrostatic. At 25g, this 1 month period is achieved in 70 minutes spinning. By measuring surface settlement during the consolidation period, previous work (Ghahremani and Brennan, 2009) back-calculated a mean coefficient of consolidation c_v for each model tested. This showed, unsurprisingly, that the largest lumps ("big cubes") produce a faster dissipation than the smaller "grated" lumps, in this case by a factor of approximately 2 (Table 1).

Once the required period of consolidation had passed, cover depths above the pipeline were measured visually using photographic images including a scale , with values of H in the range 2.0 – 2.8 D. Uplift was started at the required rate, with three rates chosen being 0.6 mm/hour, 6 mm/hour and 60 mm/hour at prototype scale. Data from in situ testing e.g. T bar testing (Lehane et al., 2009) suggests that when the nondimensional group vD/c_v is greater than 10-20 then the process may be considered undrained, with drained behaviour coming when the group is less than 0.01. Table 1 shows that the velocity range tested here should cover the partially drained range up to fully undrained using conventional wisdom based on homogenous material. The appropriateness of this assumption is revisited in Section 4. Uplift of the model pipeline was continued until the pipe had been extracted from the soil, taking from 3 minutes for the faster tests to over 4 hours for the slowest. Further information on centrifuge model setup and soil bed formation can be found in Ghahremani (2008).

3. Centrifuge Results

Seventeen centrifuge tests were carried out with the one month consolidation period, as listed in Table 1, comprising four with grated lumps (GR), six with small cubes (SC) and seven with big cubes (BC). Table 1 also lists the test uplift velocity v, measured soil properties submerged unit weight γ' and c_v, derived rate parameters vB/c_v and $v.D/c_v$ for use in assessing rate behaviour, measured peak uplift forces (where appropriate) P, active bearing capacity factor according to equation 2, N_c, and the strength reduction factor η back calculated using equation 1.

3.1 Influence of Lump Size

Measured pullout force per unit length P was corrected to eliminate the weight of the pipe and hanger, so it would be identical to the resistance of the soil to pipe movement (R in Equation 1). Figure 4 shows force-displacement data for tests from the slowest (Figure 4a: tests GS1, SS1 and BS1) and fastest (Figure 4b, tests GF1, SF1 and BF1) tests. In Figure 4, P has been further normalized by a term related to the weight of overlying soil $\gamma'HD$, in line with work of other authors, in order to adjust for slight variations in achieved cover depth between tests. Displacement has been normalized by pipe diameter D as mobilization distances from clay materials are often considered as a proportion of pipe diameter (e.g. (DNV, 2007) gives mobilization distances of 1 – 3 % D). Different curves in Figure 4 relate to different sizes of clay lump, as indicated. What is clear from both graphs is that increasing the size of the lumps has a clear and repeatable effect in increasing the peak normalized uplift resistance for the size of lumps tested here (cube sides = 0.47-0.98D for the big and small cubes respectively). The largest lumps which have sides that approach the dimensions of the pipeline (big cubes) have peak uplift resistance that is up to 25% greater than the resistance provided by the smallest (grated lumps) at both speeds. A similar trend is seen for the intermediate speeds as reported by (Ghahremani, 2008). This indicates that the lumpiness (or the relative lump to pipeline diameter) of the soil clearly influences uplift resistance, and that the nature of those lumps is important (at the sizes tested here).

It would be expected that the shear surface to pass through a combination of both intact lumps and weaker interfaces, and consequently that when the lumps are larger a greater proportion of shearing occurs in stronger soil (Figure 5). Alternatively, if there is a great difference between the lump and interface strength then shearing may find a preferential path around the lumps, which will be a longer detour if the lumps are larger.

Figure 4 also gives an indication of the mobilization distances, that is, the displacement required to mobilize peak pullout force. In these tests, mobilization/diameter ratios are between 40% and 80% compared to expected full scale values for local failure in intact soil of 1-3% (as reported by DNV, 2007). The same source refers to global failure tests in which lumpy backfill mobilizes five times greater mobilization distance than reconstituted clay, suggesting that displacement/D might be as high as 15%, still well below the measured values. However, mobilization distances have been noted in previous work on sandy soils to appear artificially large in centrifuge tests. Whilst the majority of centrifuge scaling laws are universally accepted, there remains debate over the scalability of mobilization distance. (Palmer et al., 2003) and (Stone and Newson, 2006) have suggested that mobilization distances measured on a centrifuge in sandy soils, where discrete shear bands form, may not scale as other displacements but may be subject to a different scaling law related to particle size. There is insufficient evidence as yet to suggest what this might be, nor experience on whether this applies also to clay soils as studied here. For this reason, mobilization distances are scaled in the conventional manner (or rather normalized by the pipe diameter, which does scale) for this work, but results are only used for self comparison and it is not recommended that the mobilization distance values reported be used more widely until this scaling is better understood.

It is seen, therefore, that there are minimal differences between mobilization distances in tests at the same speed. This implies that the dependence of mobilization distance on the exact nature of the backfill is very limited and may be negligible.

3.2 Influence of Uplift Velocity

Testing is performed at three different uplift velocities: 0.6 mm/hour, 6.0 mm/hour and 60 mm/hour. As described above, back-calculated c_v values equate the fastest test to undrained loading and the slower tests to be partially drained. Figure 6 shows normalized force-displacement graphs across the range of velocities for the largest (Figure 6a, tests BS1, BM1 and BF1) and smallest (Figure 6b, tests GS1 and GF1) lump shapes. The results clearly show that the uplift resistance is increased with increasing uplift velocity in all lumps. This data, first published by (Ghahremani, 2008), is in line with the independently derived results of (Cheuk et al., 2007) and (Wang et al., 2009). These authors also suggested that pore water suction was playing a role but were unable to quantify this.

The role of pore suction is evident in Figure 6a. The fastest test in the big cube material experiences a sharp drop in resistance at a displacement of 1.1D. This can only be caused by a sudden release of suction, and it may be seen that once this suction has been released, the soil resistance drops to the same curve as the slower tests. This data, in particular the observed sudden drop in force, confirms that excess pore pressures are playing a significant role in faster uplift events. To further quantify this, the measured pore pressures above and below the pipe are examined below.

Mobilization displacement is also apparently increased with increasing uplift velocity. However, this may also be affected by the suction. Greater displacements may be expected to open up a greater gap beneath the pipe containing only pore fluid. As displacement is further increased, the high bulk modulus of the water means that unless sufficient replacement water enters this gap, there is a corresponding large drop in pressure and consequently measured mobilization distances increasingly affected by the duration that this suction is retained.

3.3 Influence of Pore Water Suction

Seven of the seventeen tests showed evidence of having been influenced unduly by sub-pipe suctions during uplift. These were able to be identified by the measurements of pore pressure above and below the pipe, and their peak forces not used for further analysis. In Table 1 they are identified by an asterisk (tests GS2,SM1, SM2, SF2, BS3, BF2, BF3). However, these measurements also shed some light on the relationship between pore water suctions and the measured resistance. Figure 7a shows pore pressures measured above and below the pipe during a big cube test (BF3), with the hydrostatic component subtracted. Figure 7b shows the corresponding uplift forces. This test shows the greatest suction release measured in the tests series. Figure 7a shows a marked decrease in sub-pipe pore pressure as the suction builds up. Once the pipe has been displaced a distance of 0.2D, this suction is released as shown by the sudden rise in pressure in Figure 7a. Figure 7b shows that this results immediately in a drop in the uplift force being applied. Quantitatively, the suction of 8.7 kPa (Figure 7a) corresponds to the drop in uplift force of 3.3 kN/m (Figure 7b). If it is reasoned that this drop in force per unit length, ΔP, is equal to the product of the suction pressure released and the width of pipe over which it acts, then the data may be used to determine what proportion of the pipe width is subjected to suction. Dividing these directly comparable values from Figure 7 gives a dimension of 0.379 m (prototype scale) as the width over which the suction acts. This implies that

suction does not restrain the entire pipe width D but a reduced width of 0.6D. Similar values are recorded for other tests (Ghahremani, 2008). This implies that suction acts over a width of 0.6D in these tests, as shown in Figure 8. Figure 8a is a schematic illustration of a gap formed as the pipe approaches peak resistance. Figure 8b is a photograph of a typical test at a displacement near mobilization distance and demonstrating a gap of 0.6D, providing a visual confirmation of this empirically determined value.

This information allows approximation of the amount of force resistance contributed by suction as 0.6D × pore pressure change. Negligible suction was observed for most tests performed at the "partially drained" speeds. Affected tests are clearly identified in Table 1. This shows that while faster tests were more likely to experience suctions, this was not a predictable phenomenon and therefore common practice of ignoring suctions during uplift is appropriate and not unconservative.

4. Strength Reduction Factor

The strength reduction factor η presented in (DNV, 2007) is given the suggested limit values of 0.55 and 0.8 and a recommended value of 0.65. It may be inferred that none of the tests on remoulded clay, on which these values were based, were able to mobilize over 80% of even their remoulded strength. The guidance on selection of η is vague due to lack of certainty over the cause of this, but the design resistance is rather sensitive to this parameter. This is partially because η is a linear multiplier, i.e. a 10% reduction in η causes a 10% reduction in local-mechanism load capacity (Equation 1), but also because η is not a factor in the global load capacity so this can also affect whether a global or a local mechanism is likely to predominate. This seems a significant dependence on a potentially obscure parameter and serves to indicate the importance of getting the strength reduction factor to be the most appropriate value for the site conditions. Therefore, evaluating the performance of blocky backfill in these terms is instructive and necessary.

As all centrifuge tests were carried out with depth of cover H greater than the maximum at which a global failure might be expected then the failure mechanisms in all the centrifuge tests were of the local mode and may be analysed as such. Therefore, Equation 1 may be used to evaluate the value of η acting in each test. Rearranging Equation 1 (and taking soil resistance R as equal to the measured pullout force corrected for pipe weight P) gives Equation 3, in which the measured pullout

force P is divided by the theoretical value of N_c according to Equation 2, the pipe diameter D of 0.635 m and a value of undrained shear strength. The value of s_u used in this analysis has been chosen to be the 7 kPa measured for the intact soil. This is reasoned to be the strength of the intact lumps themselves, and therefore comparable to the s_u value that would be measured from an in situ site investigation. The soil in this study was not of high sensitivity, but if the soil within the lumps is considered to be undisturbed then the intact shear strength may be the appropriate value.

$$\eta = \frac{P}{N_c D s_u} \qquad \text{Equation 3}$$

Using Equation 3, the values of η back calculated from the centrifuge tests are determined and plotted in Figure 9. They are plotted as a function of the dimensionless group based on the commonly used parameter for distinguishing between drained and undrained loading, here formulated as $v.B/c_v$ where B is characteristic lump size and is taken as indicative of a typical drainage path length. As well as identifying drainage characteristics, higher values of B indicate a material with a greater proportion of the matrix being stronger lumps compared to weaker interfaces (Figure 5). Values for c_v are determined based on back calculation of pre-uplift consolidation data (Ghahremani and Brennan, 2009) and reported in Table 1. Values of η obtained are bounded by limits of 0.35 to 0.6, indicating that as the parameter η could be rather less in blocky backfill than in reconstituted soils representing homogenous backfill in DNV, where a range of 0.55 to 0.8 is given.

A key feature of Figure 9 is that at moderate values of $v.B/c_v$ then the existing DNV values appear to be satisfactory, in that the back calculated values of η are close or inside with suggested range, albeit at the lower end. However, at low values of $v.B/c_v$, where small lumps and low velocities are present, values of η appear to be noticeably lower than the recommended range. It is suggested that in this range, the soil behaviour has departed from the assumed undrained behaviour and is beginning to experience a partially drained response, due to the short drainage path lengths in the lumpy material relative to the rate of uplift. This appears to be the case for values of $v.B/c_v$ less than 0.05,

Figure 9 also shows two low η values at the higher-rate end of the graph. It is possible that this could be affected by viscosity-related rate effects due to a comparatively high rate of uplift, although this is less well understood than the low rate partial drainage. However, although Figure 9 shows an encouraging trend that is helpful in understanding the test data, for design purposes it has limited use

because the independent variables v, B and c_v for the lumpy material would not be known or difficult to determine in the field. Of these variables, the one that would be estimated with the greatest confidence would be lump size B, which could be controlled by jet configuration and checked visually post-lay. Figure 10 therefore presents the back-calculated values of η against the corresponding lump size normalized by the diameter of the pipe, as it is the pipe diameter that controls failure mechanism (Figure 1) and hence whether lumps are considered big or small.

Figure 10 shows some scatter between data points, but a sufficiently clear trend for further use. Therefore, a best fit straight line is included, together with limit values at ±0.05 either side. These limits encompass almost all the data. These limits may be expressed as (Equation 4a and 4b):

$$\eta_{upper} = 0.17\frac{B}{D} + 0.42 \qquad \text{Equation 4a}$$

$$\eta_{lower} = 0.17\frac{B}{D} + 0.32 \qquad \text{Equation 4a}$$

Should they be extrapolated well beyond the lump sizes tested, the intact soil condition is approached and the values of η increase towards the DNV values at B/D values of 1.4 at the lower limit and 2.5 at the upper limit – i.e. effectively intact backfill. This appears to be a useful starting point for a more informed treatment of lumpy backfills, albeit based on one value of pipe diameter and one clay type.

5. Conclusions

Uplift resistance estimations for buried pipes in clay soils are commonly based on analysis and testing considering the soil to be either undisturbed or, at best, remoulded. The installation process is highly disruptive and may cause the seabed to cut up into smaller lumps, which then form the backfill material above the pipe. As each lump has strength comparable to the intact soil but the interfaces between lumps will be rather reduced, it is difficult to assess the actual resistance that the backfill will provide to pipe uplift.

A series of centrifuge tests on different size lumps of reconsolidated lumpy clay backfill has shown that the uplift resistance in this material is governed strongly by the size of the lumps and, to a lesser

extent, by the rate at which displacement occurs. Mobilization distance does not appear to be significantly affected.

Pore pressures measured above and below the pipe showed that suctions can occur during testing. The resulting increase in uplift resistance was quantified as equalling the pore pressure difference acting across 0.6 of pipe diameter, but this was too unreliable to be relied on for any resistance in practice. Suction-affected tests were hence identified and eliminated from further analysis here, and care should be taken when interpreting test data in clay if pore pressure data is not presented.

Measured soil resistance is interpreted in terms of the strength reduction factor η, defined in the recommended practice document (DNV, 2007) as a parameter to correct between undrained shear strengths measured during site investigation and those that appear to act during uplift events. Values for the lumpy clay backfills tested here showed values of η at the lower limit expected based on the more intact clay data. This correlated well with a nondimensional drainage based parameter based on uplift velocity v, backfill coefficient of consolidation c_v and a characteristic lump size B. It was also seen that for values of $v.B/c_v$ below 0.05 then η became noticeably reduced in the lumpy backfill. However, it is appreciated that for practical purposes it is difficult to know the values of v and c_v, and therefore a correlation between η and lump size/pipe diameter was also proposed as an improvement on existing recommendations when applied to lumpy clay backfills.

Acknowledgements

The centrifuge programme and construction of the model pipe was carried out with the assistance of University of Dundee technical staff Mark Truswell, Michael McKernie, Colin Stark, Charlie Webster and Ernie Kuperus, whose contributions are acknowledged with thanks.

References

Bransby, M.F., Newson, T.A., Brunning, P., 2002. The upheaval capacity of pipelines in jetted clay backfill. International Journal of Offshore and Polar Engineering 12 (4), 280-287.

Cheuk, C.Y., Take, W.A., Bolton, M.D., Oliveira, J., 2007. Soil restraint on buckling oil and gas pipelines buried in lumpy clay fill. Engineering Structures 29 (6), 973-982.

DNV, 2007. Global buckling of submarine pipelines, Recommended Practice. Det Norske Veritas.

Eiksund, G., Langø, H., Øiseth, E., 2013. Full-scale test of uplift resistance of trenched pipes. International Journal of Offshore and Polar Engineering 23 (4), 298-306.

Ghahremani, M., 2008. Pipe uplift resistance in blocky clays. MSc thesis, University of Dundee UK.

Ghahremani, M., Brennan, A.J., 2009. Consolidation of lumpy clay backfill over buried pipelines, 28th International Conference on Ocean, Offshore and Arctic Engineering, Honolulu, USA.

Lehane, B.M., O'Loughlin, C.D., Gaudin, C., Randolph, M.F., 2009. Rate effects on penetrometer resistance in kaolin. Geotechnique 59 (1), 41-52.

Maltby, T.C., Calladine, C.R., 1995. An investigation into upheaval buckling of buried pipelines 2: Theory and analysis of experimental observations. International Journal of Mechanical Sciences 37 (9), 965-983.

Martin, C.M., White, D.J., 2012. Limit analysis of the undrained bearing capacity of offshore pipelines. Geotechnique 62 (9), 847-863.

Ng, C.W.W., Springman, S.M., 1994. Uplift resistance of buried pipelines in granular materials. Centrifuge 94, 753-758.

Palmer, A.C., White, D.J., Baumgard, A.J., Bolton, M.D., Barefoot, A.J., Finch, M., Powell, T., Faranski, A.S., Baldry, J.A.S., 2003. Uplift resistance of buried submarine pipelines: comparison between centrifuge modelling and full-scale tests. Geotechnique 53 (10), 877-883.

Schaminee, P.E.L., Zorn, N.F., Schotman, G.J.M., 1990. Soil response for pipeline upheaval buckling analyses: full scale laboratory tests and modelling, 22nd Offshore Technology Conference, Houston, USA, pp. 563-572.

Schofield, A.N., 1980. Cambridge geotechncial centrifuge operations. Geotechnique 30 (3), 227-268.

Stone, K.J.L., Newson, T.A., 2006. Uplift resistance of buried pipelines: An investigation of scale effects in model tests, in: Ng, C.W.W., Zhang, L.M., Wang, Y.H. (Eds.), Physical Modelling in Geotechnics - 6th ICPMG '06, Vol 1, pp. 741-746.

Trautmann, C.H., Orourke, T.D., Kulhawy, F.H., 1985. Uplift force-displacement response of buried pipe. Journal of Geotechnical Engineering-Asce 111 (9), 1061-1076.

Wang, J., Haigh, S.K., Thusyanthan, I., 2009. Uplift resistance of buried pipelines in blocky clay backfill, 19th International Offshore and Polar Engineering Conference, Osaka.

Tables

Table 1. Salient test data (GR = grated lumps, SC = small cubes, BC = big cubes)

Test ID	Lumps	B (mm)	v (mm/hr)	γ' (kN/m^3)	H/D	c_v (m^2/yr)	vD/ c_v	vB/ c_v	P (kN/m)	N_c	η
GS1	GR	50	0.6	6.65	2.58	18	0.185	0.015	17.02	9.57	0.40
GS2	GR	50	0.6	6.59	2.61	18	0.185	0.015	16.43*		
GF1	GR	50	60	6.45	2.83	19	17.566	1.383	22.02	9.63	0.51
GF2	GR	50	60	5.72	2.55	19	17.566	1.383	21.98	9.57	0.52
SS1	SC	300	0.6	6.63	2.73	40	0.083	0.039	20.28	9.61	0.47
SS2	SC	300	0.6	6.61	2.84	45	0.074	0.035	19.29	9.63	0.45
SM1	SC	300	6	6.42	2.42	61	0.547	0.258	19.76*		
SM2	SC	300	6	6.48	2.03	32	1.043	0.493	22.69*		
SF1	SC	300	60	6.68	2.5	52	6.418	3.032	23.5	9.55	0.55
SF2	SC	300	60	6.53	2.51	42	7.947	3.754	17.22*		
BS1	BC	600	0.6	6.66	2.37	49	0.068	0.064	19.1	9.52	0.45
BS2	BC	600	0.6	6.6	2.31	27	0.124	0.117	17.76	9.50	0.42
BM1	BC	600	6	6.62	2.54	23	1.451	1.371	21.54	9.56	0.51
BS3	BC	600	0.6	6.23	2.62	37	0.090	0.085	18.95*		
BF1	BC	600	60	6.95	2.44	49	6.811	6.436	23.9	9.54	0.56
BF2	BC	600	60	6.12	2.56	52	6.418	6.065	26.93*		
BF3	BC	600	60	6.89	2.51	70	4.768	4.505	19.07*		

1 *Uplift forces affected by excessive suction

2

Figure Captions

Figure 1. Schematic illustration of uplift mechanisms a) local failure b) global failure

Figure 2. 25 mm diameter model pipeline a) photograph; b) schematic showing internal pressure transducers for measuring crown and bottom pore pressures

Figure 3 a) Big cubes, b) small cubes, c) grated lumps

Figure 4. Normalized pullout force vs. normalized displacement as a function of lump size at a) 60 mm/hr and b) 0.6 mm/hr

Figure 5 Schematic of relative proportion of lumps and interfaces involved in shearing a) larger and b) smaller lumps

Figure 6 Normalized force vs normalized displacement as a function of uplift velocity for a) large lumps and b) small lumps

Figure 7. Suction-affected test, 6 mm/hr uplift rate applied to a pipe in big cubes, in terms of a) pore pressures measured above and below the pipe, and b) resistance per unit length

Figure 8. Sub-pipe voids a) schematic and b) during a test, at displacement approaching mobilization distance

Figure 9. Values of η back calculated from centrifuge data as a function of nondimensional $v.B/c_v$

Figure 10. Values of η as a function of characteristic lump size relative to pipe diameter

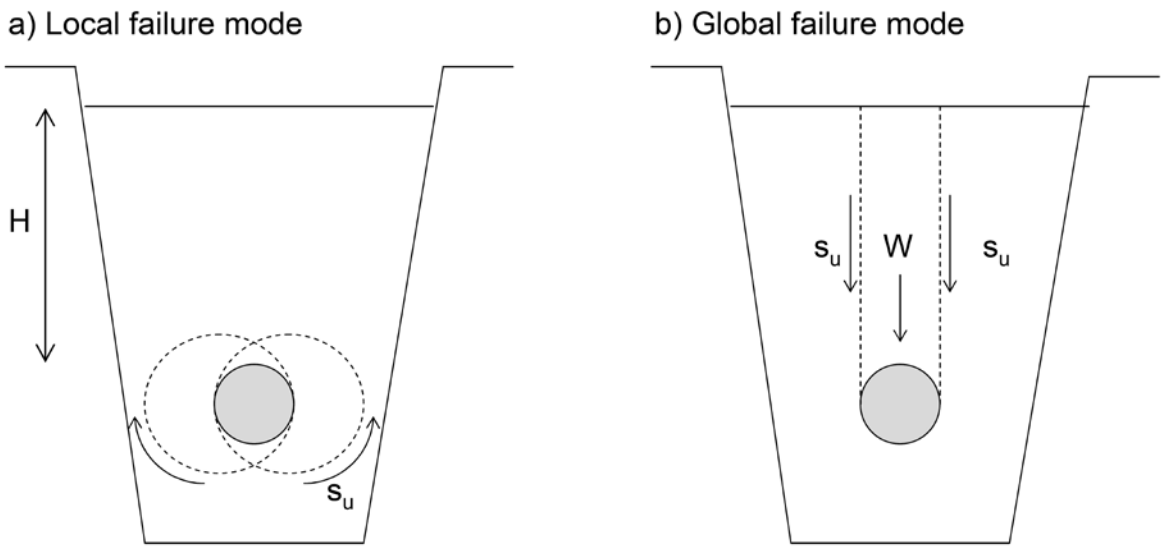

1

2 **Figure 1. Schematic illustration of uplift mechanisms a) local failure b) global failure**

3

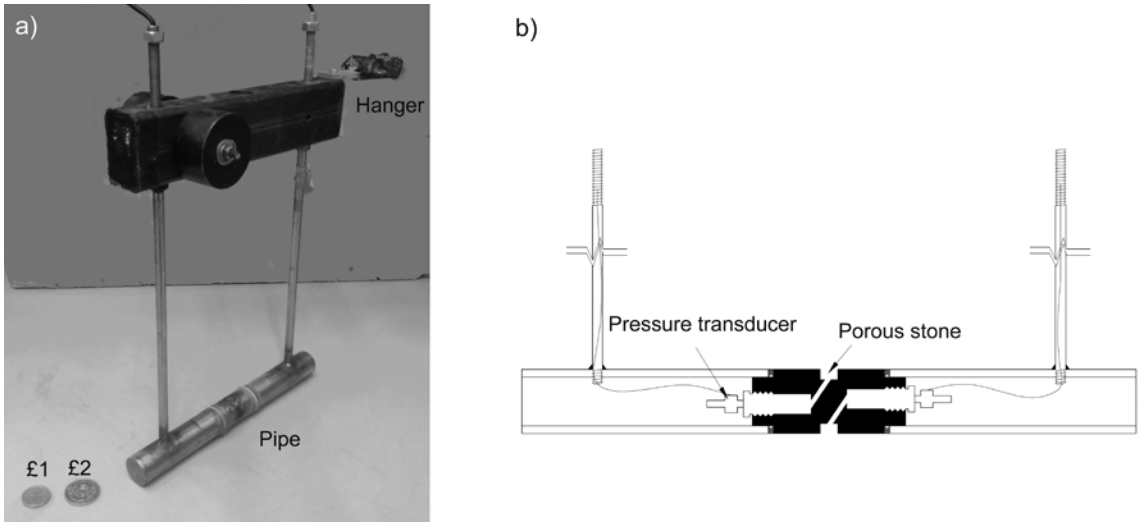

Figure 2. 25 mm diameter model pipeline a) photograph; b) schematic showing internal pressure transducers for measuring crown and bottom pore pressures

a) Big cubes

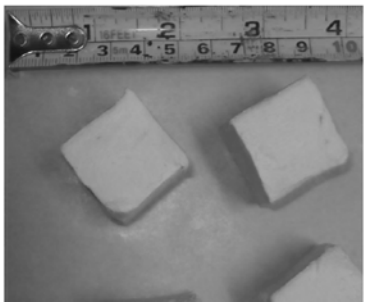

b) Small cubes

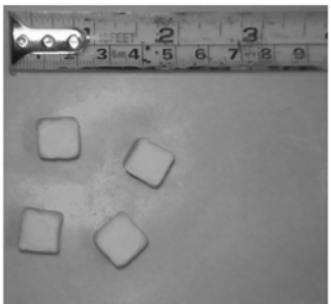

c) Grated lumps

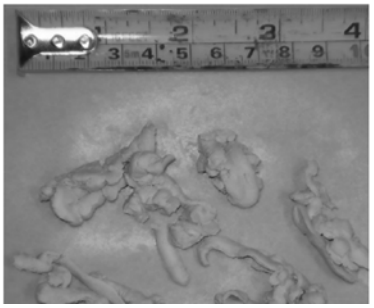

Figure 3 a) Big cubes, b) small cubes, c) grated lumps

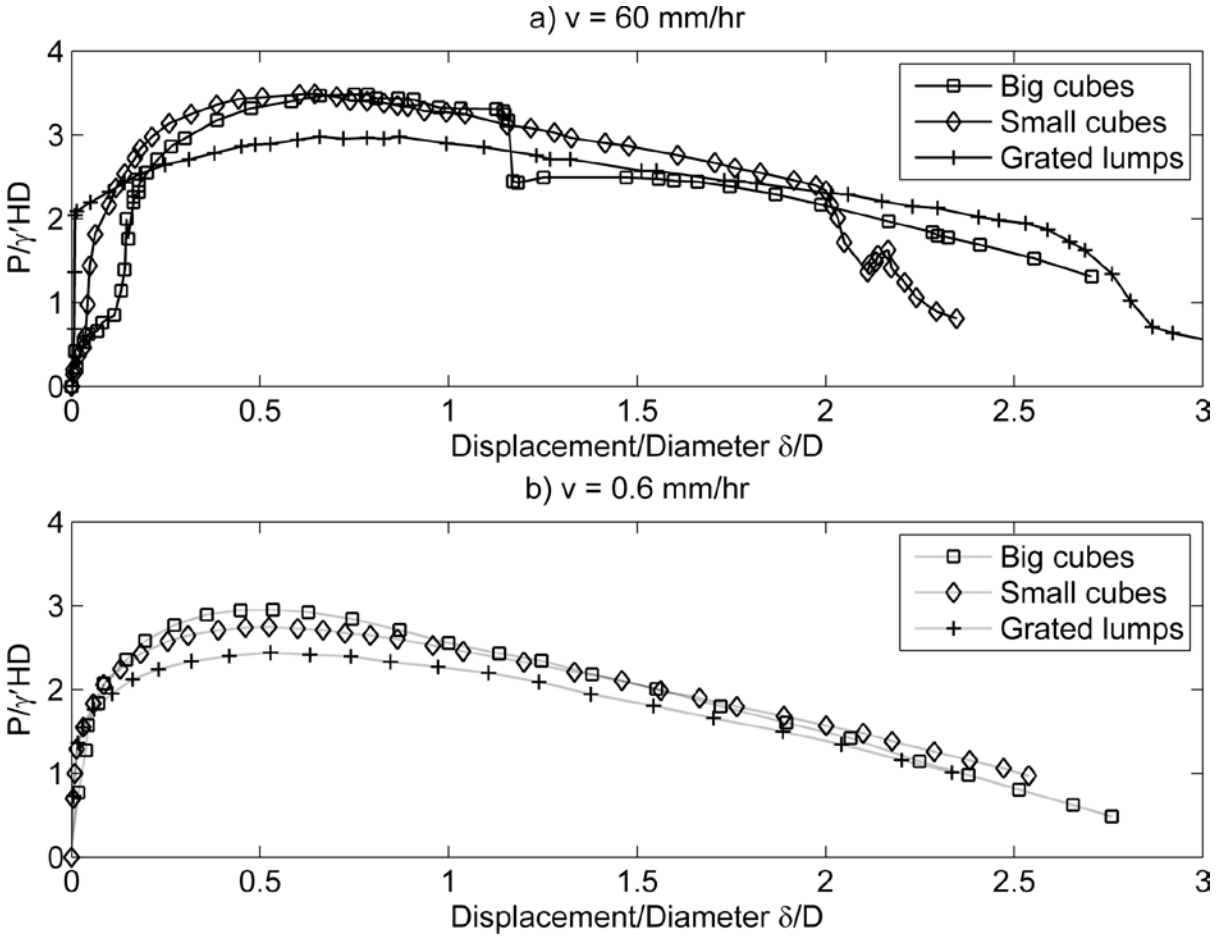

Figure 4. Normalized pullout force vs. normalized displacement as a function of lump size at a) 60 mm/hr and b) 0.6 mm/hr

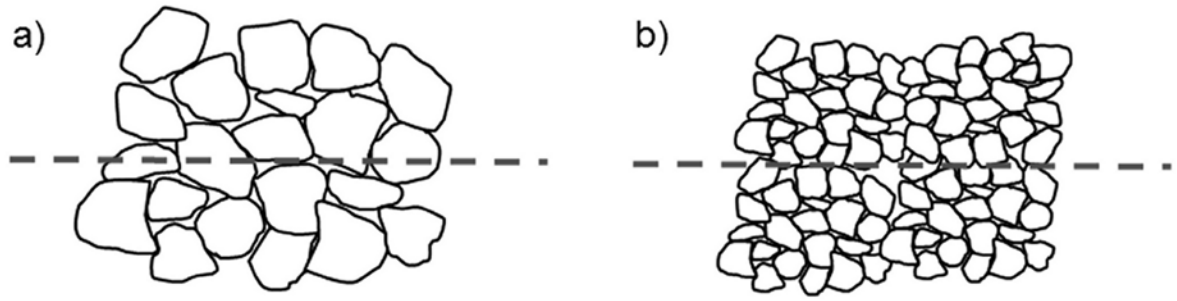

Figure 5 Schematic of relative proportion of lumps and interfaces involved in shearing a) larger and b) smaller lumps

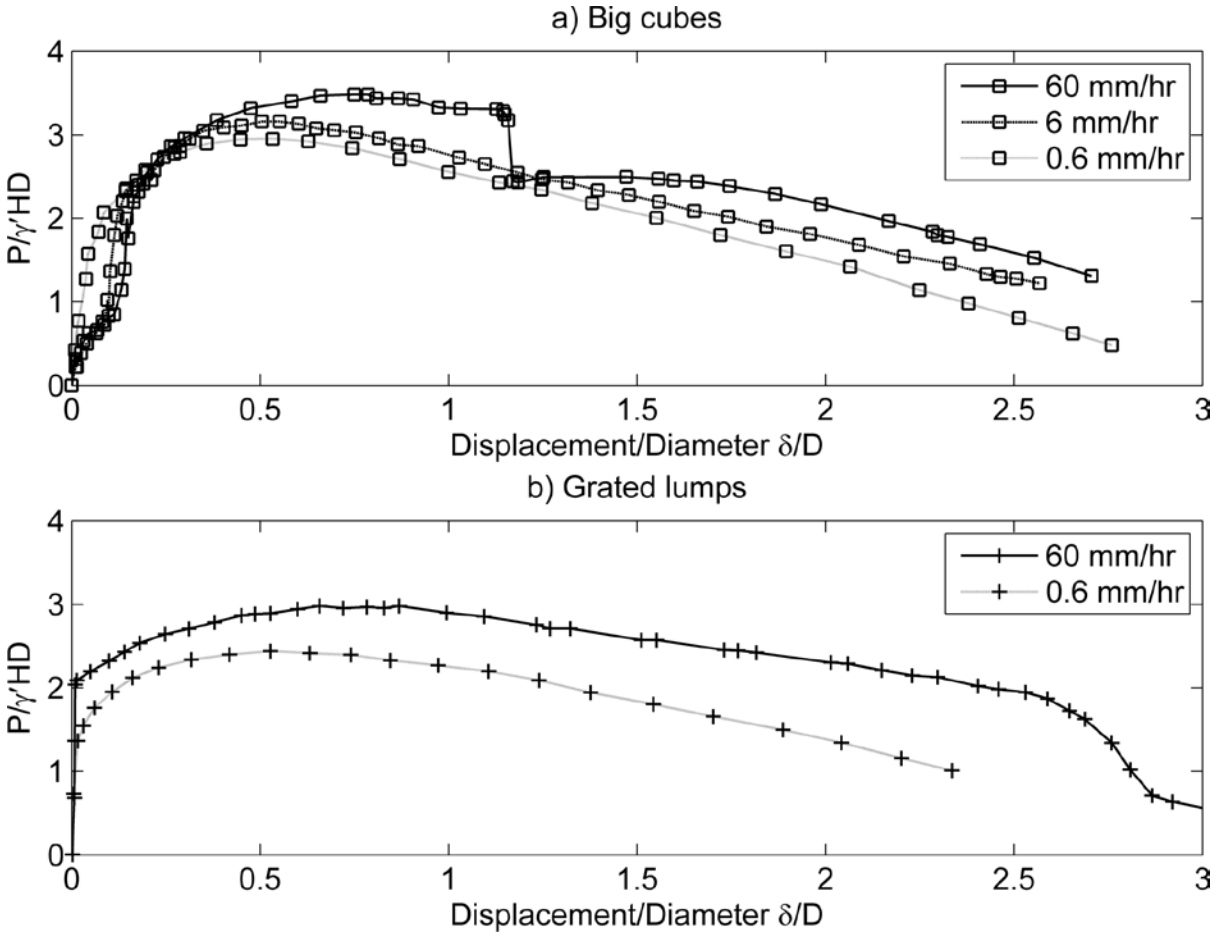

Figure 6 Normalized force vs normalized displacement as a function of uplift velocity for a) large lumps and b) small lumps

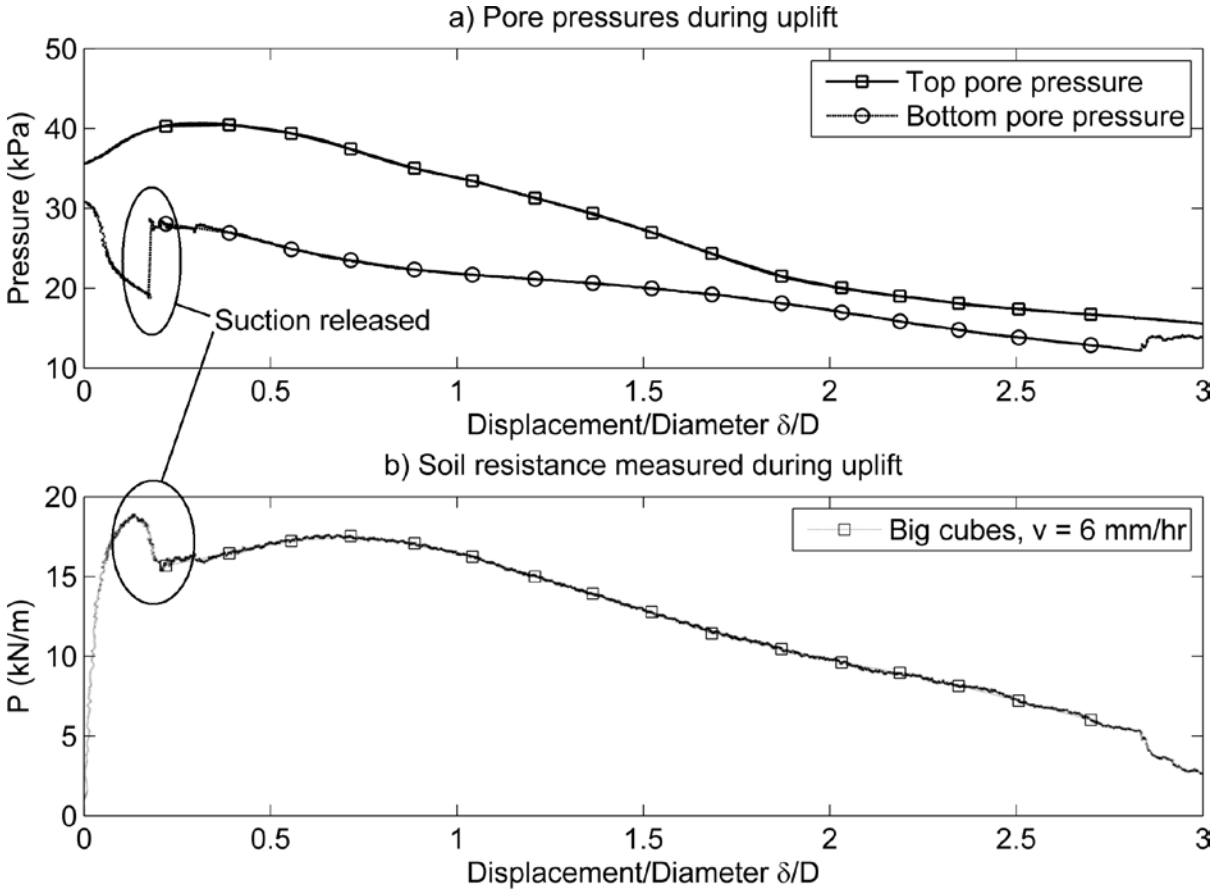

Figure 7. Suction-affected test, 6 mm/hr uplift rate applied to a pipe in big cubes, in terms of a) pore pressures measured above and below the pipe, and b) resistance per unit length

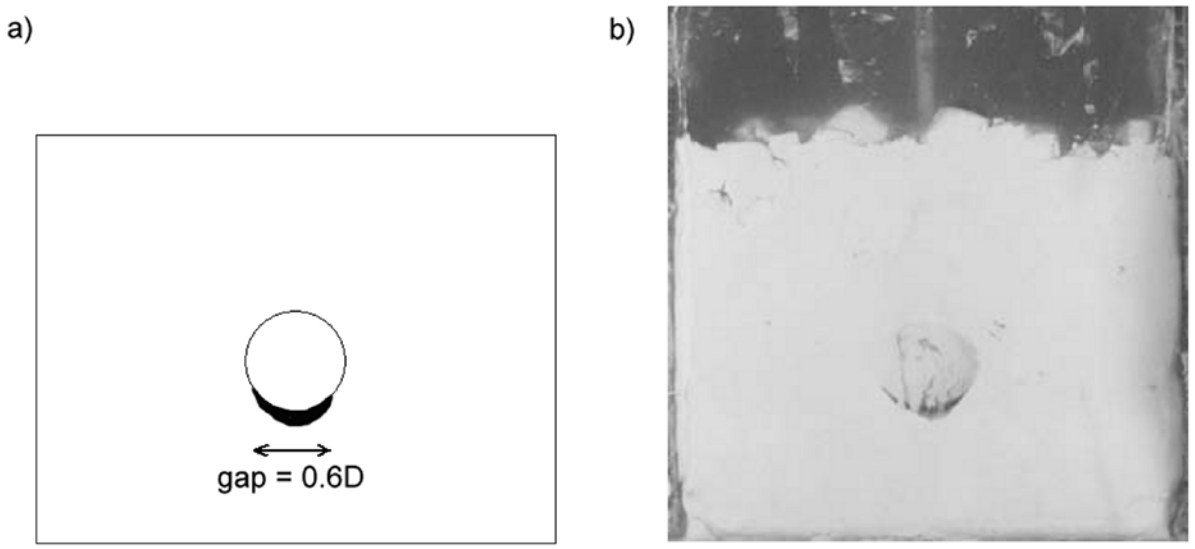

Figure 8. Sub-pipe voids a) schematic and b) during a test, at displacement approaching mobilization distance

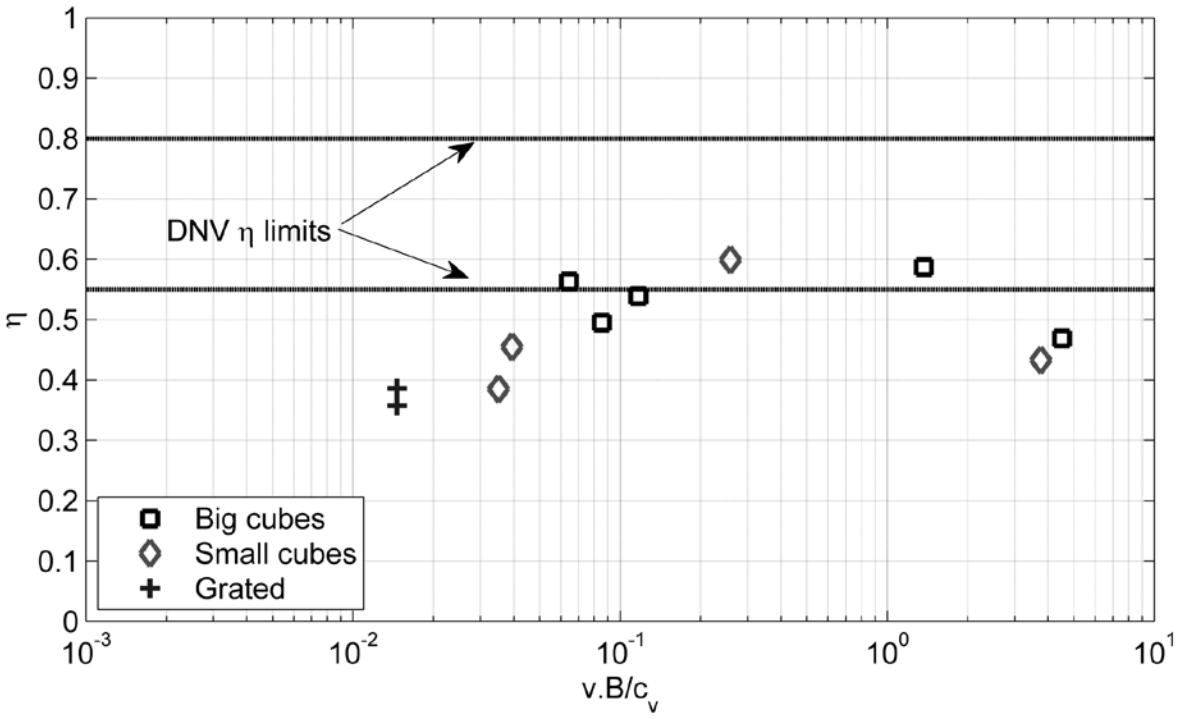

Figure 9. Values of η back calculated from centrifuge data as a function of nondimensional $v.B/c_v$

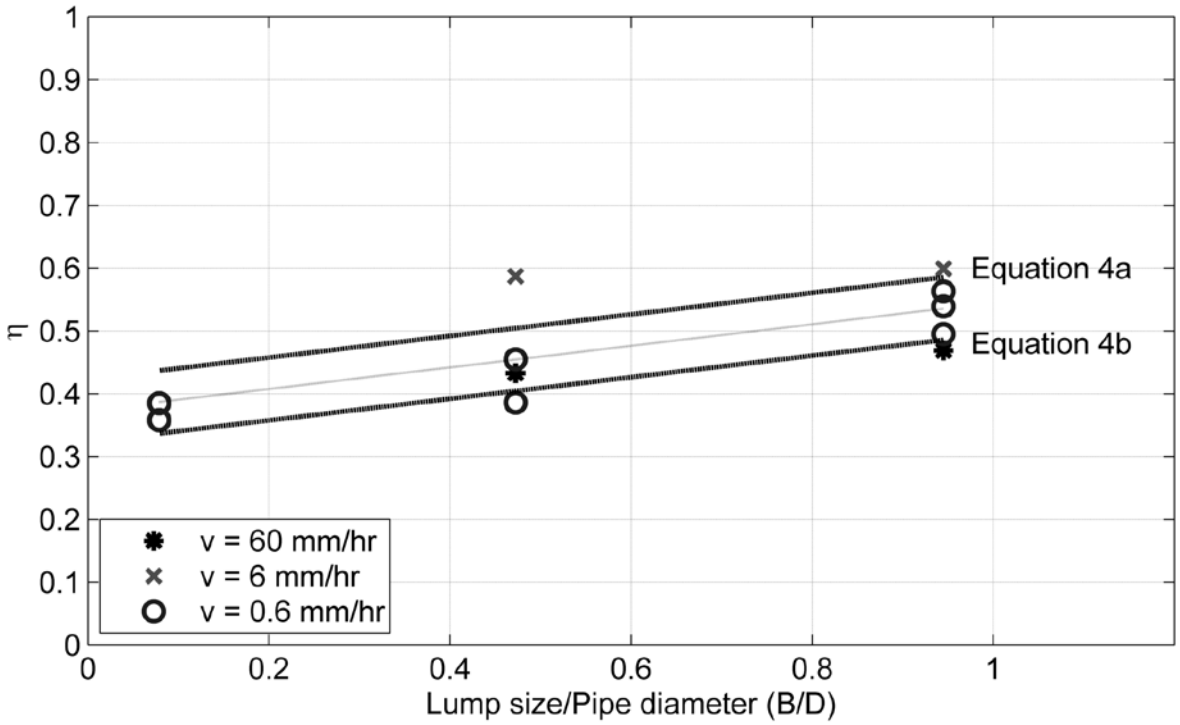

Figure 10. Values of η as a function of characteristic lump size relative to pipe diameter